Centrum voor Wiskunde en Informatica

REPORT*RAPPORT*

MAS

Modelling, Analysis and Simulation

Modelling, Analysis and Simulation

Discontinuous Galerkin discretisation with embedded boundary conditions

P.W. Hemker, W. Hoffmann, M.H. van Raalte

REPORT MAS-R0301 MARCH 31, 2003

CWI is the National Research Institute for Mathematics and Computer Science. It is sponsored by the Netherlands Organization for Scientific Research (NWO).
CWI is a founding member of ERCIM, the European Research Consortium for Informatics and Mathematics.

CWI's research has a theme-oriented structure and is grouped into four clusters. Listed below are the names of the clusters and in parentheses their acronyms.

Probability, Networks and Algorithms (PNA)

Software Engineering (SEN)

Modelling, Analysis and Simulation (MAS)

Information Systems (INS)

P.O. Box 94079, 1090 GB Amsterdam (NL)
Kruislaan 413, 1098 SJ Amsterdam (NL)
Telephone +31 20 592 9333
Telefax +31 20 592 4199

ISSN 1386-3703

Discontinuous Galerkin Discretisation with Embedded Boundary Conditions

P.W. Hemker[*,**], W. Hoffmann[**] and M.H. van Raalte[*,**]

[*] *CWI, P.O. Box 94079, 1090 GB Amsterdam, The Netherlands*

[**] *KdV Institute for Mathematics, University of Amsterdam*
Plantage Muidergracht 24, 1018 TV Amsterdam, The Netherlands

ABSTRACT

The purpose of this paper is to introduce discretisation methods of discontinuous Galerkin type for solving second order elliptic PDEs on a structured, regular rectangular grid, while the problem is defined on a curved boundary. The methods aim at high-order accuracy and the difficulty arises since the regular grid cannot follow the curved boundary.

Starting with the Lagrange multiplier formulation for the boundary conditions, we derive variational forms for the discretisation of 2-D elliptic problems with embedded Dirichlet boundary conditions. Within the framework of structured, regular rectangular grids, we treat curved boundaries according to the principles that underlie the discontinuous Galerkin method. Thus, the high-order DG-discretisation is adapted in the cells with embedded boundaries. We give examples of approximation with tensor products of cubic polynomials.

As an illustration, we solve a convection dominated boundary value problem on a complex domain. Although, of course, it is impossible to accurately represent a boundary layer with a complex structure by means of a cubic polynomial, the boundary condition treatment appears quite effective in handling such complex situations.

2000 Mathematics Subject Classification: 65N50; 65N99
Keywords and Phrases: DG discretisation, structured grid, irregular boundary, embedded boundary
Note: This work was carried out under project MAS2.1 "Computational Fluid Dynamics".

1. Introduction

The purpose of this paper is to introduce methods of discontinuous Galerkin type for solving second order elliptic PDEs on a structured, regular rectangular grid while the problem is defined on a curved boundary. The methods aim at high-order accuracy and the difficulty arises because the regular grid cannot follow the curved boundary.

Earlier, several techniques were proposed to handle boundary conditions on irregular, curvilinear boundaries. The most convenient certainly is the FEM, where elements near the boundary are adapted to the shape of the boundary curve. Generally, this results in an unstructured grid. This relatively straightforward technique can be applied up to arbitrarily high-order of accuracy and delivers good results.

In contrast, finite difference methods are usually applied on regular grids. Here, curved boundaries are treated by locally adapted finite differences as, e.g., Shortley-Weller approximation [4, Sect.4.8]. Generally, such discretisations are not used for higher orders of accuracy.

A more recent technique for treatment of complex boundaries on orthogonal grids, in two or three dimensions, is the Embedded Curved Boundary (ECB) method. Here –usually in the context of the discretisation of conservation laws– piecewise linear segments are embedded in the grid to represent the boundary. The method is also used, e.g., for solutions across interfaces [7, 8]. In many cases the ECB method shows clear advantages compared to the traditional stair-step method [10] but no higher-order accuracy than order two can be expected.

Higher order may be obtained by Immersed Boundary Methods (IBM) [11, 12, 13, 16], e.g., in pseudo-spectral codes [3], where the presence of a boundary within the computational domain is simulated by specifying a body force term, without altering the computational grid. This technique is very flexible as it allows for bodies and interfaces of almost arbitrary shape. The method is quite popular in situations with interfaces and rather complex geometries [9] and e.g., elastic boundaries [15]. Usually the method is applied so as to maintain second order accuracy (first order near the boundaries). However, fourth order convergence rates are reported in [2], where the same methodology is used with PDEs for thin flexible membranes in an incompressible fluid domain.

In contrast with the above methods, we take the Lagrange multiplier formulation of the boundary conditions as a starting point, in the same manner as used in [14] or in the derivation of the discontinuous Galerkin discretisation. Within the framework of structured, regular rectangular grids we introduce the treatment of curved boundaries in full agreement with the principles that lead to the discontinuous Galerkin method. We apply high-order DG-discretisation in the interior and adapt the method in the cells with embedded boundaries. The order of approximation of the boundary condition corresponds with the accuracy of the DG-method. In the present paper we give examples of approximation with tensor products of cubic polynomials.

In [6] we explained why the treatment of this cubic polynomial case is the basis for higher-order approximation. In DG discretisation, information exchange over the interior cell boundaries is restricted to function values and normal fluxes. At the endpoints of an interval, function values and fluxes are determined by four independent parameters, that correspond with the four degrees of freedom in the cubic polynomial approximation on a cell. Higher-order approximation can be achieved by additional bubble functions with vanishing values and derivatives at the cell boundary. In the multi-dimensional case, on a structured rectangular grid, the same principle holds with tensor-products for approximation.

For the treatment of the embedded boundary conditions, we give in Section 2 of this paper an exposition of the weak forms used for the different discretisation alternatives. In Section 3 we start with simple experiments in one and two dimensions to see the differences between the various methods. In section 4 we identify the discrete function spaces in which the approximate solution is found. In the last section we solve a convection-dominated equation on an irregular domain, partitioned into only two cells. We show how well, on this mesh, a complex problem can be solved with a piecewise cubic approximation.

2. Weak forms for the Poisson equation

2.1 The Lagrange multiplier form for the embedded boundary problem

To apply DG-methods for structured rectangular grids on complicated domains, we are interested in solving an elliptic second order problem $Lu = f$ on a fictitious open domain $\widehat{\Omega}$, which is larger than the open domain Ω on which the elliptic BVP is originally defined. The solution u on Ω is determined by the Dirichlet boundary condition $u = u_0$ on $\partial\Omega$, the boundary of Ω, and we want to discretize the problem on a fictitious domain $\widehat{\Omega} \supset \Omega$. For this purpose we assume that the solution u on Ω allows a sufficiently smooth extension, u, defined on $\widehat{\Omega}$, solving $Lu = f$. Of course, this excludes certain types of singularities near the boundary.

For sake of simplicity, in this initial treatment we assume $\widehat{\Omega}$ to be the unit cube and we consider the Poisson equation with an embedded Dirichlet boundary condition as follows: let $\widehat{\Omega}$ be the open unit cube, with boundary $\partial\widehat{\Omega}$, which consists of two non-overlapping open sub-domains, Ω and $\widetilde{\Omega}$, such that

$$\overline{\widehat{\Omega}} = \overline{\Omega} \cup \overline{\widetilde{\Omega}}, \qquad \text{and} \qquad \Omega \cap \widetilde{\Omega} = \emptyset, \tag{2.1}$$

where $\widetilde{\Omega}$ is the fictitious part of the domain $\widehat{\Omega}$. We now consider the boundary value problem consisting of the Poisson equation defined on the whole of $\widehat{\Omega}$ and Dirichlet boundary conditions on $\partial\Omega$, the boundary of Ω:

$$Lu \equiv -\Delta u = f \ \text{ on } \ \widehat{\Omega}, \qquad \text{and} \qquad u = u_0 \ \text{ on } \ \Gamma_D = \partial\Omega, \tag{2.2}$$

under the assumption that the solution u on Ω, has a sufficiently smooth continuation to $\widetilde{\Omega}$, satisfying the Poisson equation on the whole of $\widehat{\Omega}$.

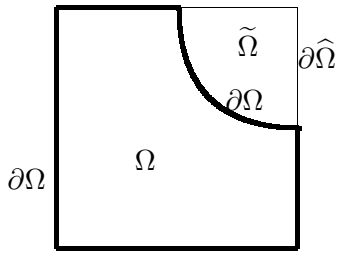

Figure 1: The domain of interest, Ω and the fictitious part, $\widetilde{\Omega}$, make the domain $\widehat{\Omega} = \Omega \cup \widetilde{\Omega}$.

To arrive at the corresponding weak formulation of the Poisson equation with 'embedded' Dirichlet boundary condition, we multiply the left- and right-hand side of (2.2) with a sufficiently smooth function v, and integrate over the domain $\widehat{\Omega}$, to get:
find $u \in H^1(\widehat{\Omega})$ such that

$$(\nabla u, \nabla v)_{\widehat{\Omega}} - \langle \mathbf{n} \cdot \nabla u, v \rangle_{\partial\widehat{\Omega}} = (f, v)_{\widehat{\Omega}} \qquad \forall v \in H^1(\widehat{\Omega}), \tag{2.3}$$
$$\text{under the constraint that } u = u_0 \text{ on } \partial\Omega.$$

By the Lagrange multiplier theorem, the following formulation is equivalent to (2.3): find $u \in H^1(\widehat{\Omega})$ and $\overline{p} \in H^{-1/2}(\partial\Omega)$ such that

$$\begin{aligned} &(\nabla u, \nabla v)_{\widehat{\Omega}} - \langle \mathbf{n} \cdot \nabla u, v \rangle_{\partial\widehat{\Omega}} + \langle \overline{p}, v \rangle_{\partial\Omega} = (f, v)_{\widehat{\Omega}} && \forall v \in H^1(\widehat{\Omega}), \\ &\langle q, u \rangle_{\partial\Omega} = \langle q, u_0 \rangle_{\partial\Omega} && \forall q \in H^{-1/2}(\partial\Omega). \end{aligned} \tag{2.4}$$

We call this the *Lagrange multiplier form* of the embedded boundary problem. We see that, if u satisfies the Poisson equation (2.2) and the embedded Dirichlet boundary condition, the Lagrange multiplier $\overline{p}$ in (2.4) vanishes.

2.2 The weak form for boundaries along gridlines
In the classical case that $\widetilde{\Omega} = \emptyset$, we can combine the boundary terms in (2.4), in order to obtain

$$\begin{aligned} &(\nabla u, \nabla v)_{\widehat{\Omega}} - \langle p, v\rangle_{\partial\widehat{\Omega}} = (f, v)_{\widehat{\Omega}} && \forall v \in H^1(\widehat{\Omega}), \\ &\langle q, u\rangle_{\partial\Omega} = \langle q, u_0\rangle_{\partial\Omega} && \forall q \in H^{-1/2}(\partial\Omega), \end{aligned}$$

with $p = \mathbf{n}\cdot\nabla u - \overline{p}$ on $\partial\Omega = \partial\widehat{\Omega}$.
This leads to a *hybrid* form of (2.2) with Dirichlet BCs: find $u \in H^1(\widehat{\Omega})$ and $p \in H^{-1/2}(\partial\Omega)$ such that

$$(\nabla u, \nabla v)_{\widehat{\Omega}} - \langle p, v\rangle_{\partial\widehat{\Omega}} - \langle q, u\rangle_{\partial\Omega} = (f, v)_{\widehat{\Omega}} - \langle q, u_0\rangle_{\partial\Omega} \quad \forall v \in H^1(\widehat{\Omega}), q \in H^{-1/2}(\partial\Omega). \tag{2.5}$$

When u satisfies (2.2) we have $p = \mathbf{n}\cdot\nabla u$, the normal flux at the boundary $\partial\widehat{\Omega}$. Substituting this value for p, and replacing similarly the weighting function q by $q = -\sigma\mathbf{n}\cdot\nabla v$, with $\sigma = 1$ or $\sigma = -1$, leads to the weak form used in DG-methods (viz., Baumann's and the symmetric DG-method respectively). Other DG-methods (viz., IPG, NIPG) are obtained by taking $q = -\sigma\mathbf{n}\cdot\nabla v - \mu v$ with parameters σ and μ. Thus, our DG weak form reads: find $u \in H^1(\widehat{\Omega})$ such that

$$\begin{aligned} (\nabla u, \nabla v)_{\widehat{\Omega}} - \langle \mathbf{n}\cdot\nabla u, v\rangle_{\partial\widehat{\Omega}} + \sigma\,\langle \mathbf{n}\cdot\nabla v, u\rangle_{\partial\Omega} = & \\ = (f, v)_{\widehat{\Omega}} + \sigma\,\langle \mathbf{n}\cdot\nabla v, u_0\rangle_{\partial\Omega} \qquad & \forall v \in H^1(\widehat{\Omega}). \end{aligned} \tag{2.6}$$

2.3 The hybrid and the DG-form for the embedded boundary problem
Not only the Lagrange multiplier form (2.4) can be used for the embedded boundary problem, we can also apply (2.5) or (2.6). In the case $\widetilde{\Omega} \neq \emptyset$ the form (2.5) reads: find $u \in H^1(\widehat{\Omega})$ and $p \in H^{-1/2}(\partial\widehat{\Omega})$ such that

$$\begin{aligned} (\nabla u, \nabla v)_{\widehat{\Omega}} - \langle p, v\rangle_{\partial\widehat{\Omega}} - \langle q, u\rangle_{\partial\Omega} = (f, v)_{\widehat{\Omega}} - \langle q, u_0\rangle_{\partial\Omega}\,, & \\ \forall v \in H^1(\widehat{\Omega}), q \in H^{-1/2}(\partial\Omega). & \end{aligned} \tag{2.7}$$

which we call the *hybrid* form of the interior boundary problem. In the case $\widetilde{\Omega} \neq \emptyset$, equation (2.6) is written: find $u \in H^1(\widehat{\Omega})$ such that

$$\begin{aligned} (\nabla u, \nabla v)_{\widehat{\Omega}} - \langle \mathbf{n}\cdot\nabla u, v\rangle_{\partial\widehat{\Omega}} + \sigma\,\langle \mathbf{n}\cdot\nabla v, u\rangle_{\partial\Omega} = & \\ = (f, v)_{\widehat{\Omega}} + \sigma\,\langle \mathbf{n}\cdot\nabla v, u_0\rangle_{\partial\Omega} \qquad & \forall v \in H^1(\widehat{\Omega}), \end{aligned} \tag{2.8}$$

which we call the *DG-form* (the Baumann-Oden weak form if $\sigma = 1$ or the symmetric form if $\sigma = -1$) of the interior boundary problem. Notice that this symmetric weak form is not symmetric anymore if $\Omega \neq \widehat{\Omega}$.

3. Numerical experiments in one and two dimensions

3.1 Numerical experiments on one-dimensional problems

To see the difference in practice, we first study the three weak forms (2.4), (2.7) and (2.8) for a simple one-dimensional problem. On the unit interval $\widehat{\Omega} = (0,1)$ we consider the Poisson equation with homogeneous Dirichlet boundary conditions:

$$-\frac{d^2u}{dx^2} = f, \quad \text{on} \quad \widehat{\Omega}, \quad \text{with} \quad u(d) = 0, \quad u(1) = 0, \tag{3.1}$$

where $d \in [0,1)$ and $\Omega = (d,1)$. To discretize this problem we take for test and trial spaces the $(p+1)$-dimensional space $S_h(\widehat{\Omega}) = P^p(\widehat{\Omega}) \subset H^1(\widehat{\Omega})$, i.e., the space of polynomials of degree $\leq p$. We write for the approximate solution

$$u_h = \sum_{0 \leq i \leq p} c_i \phi_i(x), \quad \phi_i(x) \in S_h(\widehat{\Omega}).$$

Further, we provide the boundary spaces $Q_h(\partial\widehat{\Omega}) \subset H^{-1/2}(\partial\widehat{\Omega})$ and $Q_h(\partial\Omega) \subset H^{-1/2}(\partial\Omega)$, with the trace of polynomials on the boundary, hence $Q_h(\partial\widehat{\Omega}) = \{\psi_0(x) = (1-x)|_{x=(0,1)}$, $\psi_1(x) = x|_{x=(0,1)})\}$ and $Q_h(\partial\Omega) = \{\psi_0(x) = \frac{x-1}{d-1}|_{x=(d,1)}$, $\psi_1(x) = \frac{x-d}{1-d}|_{x=(d,1)})\}$, $d \in [0,1)$. Then we write for the approximation of the Lagrange multiplier:

$$p_h = \sum_{0 \leq i \leq 1} a_i \psi_i(x)|_{x=0,d,1}.$$

Because of the 1-D character of this example, boundary values are parameterized by only two values for both $\partial\widehat{\Omega}$ and $\partial\Omega$. Given the approximating spaces, the three forms (2.4), (2.7) and (2.8) become:

(i) In case of the *Lagrange multiplier formulation*: find $u_h \in S_h(\widehat{\Omega})$, $\overline{p}_h \in Q_h(\partial\widehat{\Omega})$ such that

$$\begin{aligned} \int_0^1 u_h' v_h' dx - \left[u_h'(1)v_h(1) - u_h'(0)v_h(0)\right] + \left[\overline{p}_h(1)v_h(1) - \overline{p}_h(d)v_h(d)\right] \\ + \left[q_h(1)u_h(1) - q_h(d)u_h(d)\right] = \int_0^1 v_h f dx, \qquad \forall v_h \in S_h(\widehat{\Omega}),\ q_h \in Q_h(\partial\widehat{\Omega}). \end{aligned} \tag{3.2}$$

(ii) in case of the *hybrid form*: find $u_h \in S_h(\widehat{\Omega})$, $p_h \in Q_h(\partial\Omega)$ such that

$$\begin{aligned} \int_0^1 u_h' v_h' dx - \left[p_h(1)v_h(1) - p_h(0)v_h(0)\right] - \left[q_h(1)u_h(1) - q_h(d)u_h(d)\right] \\ = \int_0^1 v_h f dx, \qquad \forall v_h \in S_h(\widehat{\Omega}), \quad q_h \in Q_h(\partial\widehat{\Omega}). \end{aligned} \tag{3.3}$$

(iii) whereas the *DG-formulation* reduces to: find $u_h \in S_h(\widehat{\Omega})$ such that

$$\begin{aligned} \int_0^1 u_h' v_h' dx \quad - \left[u_h'(1)v_h(1) - u_h'(0)v_h(0)\right] + \sigma\left[v_h'(1)u_h(1) - v_h'(d)u_h(d)\right] \\ = \textstyle\int_0^1 v_h f dx, \qquad \forall v_h \in S_h(\widehat{\Omega}). \end{aligned} \tag{3.4}$$

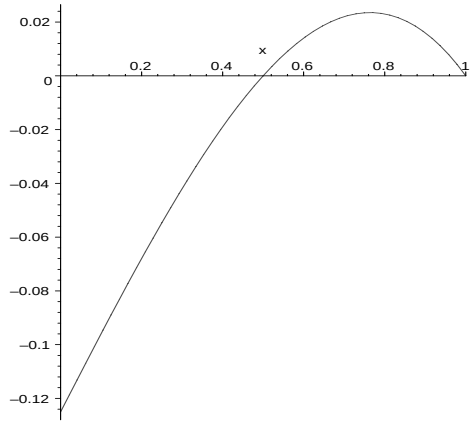

Figure 2: The solution $u(x) = -\frac{1}{6}x^3 + \frac{7}{24}x - \frac{1}{8}$ computed with the hybrid-, Lagrange- and Symmetric-Baumann- method, $\sigma = \pm 1$.

As a first experiment we check if the three discrete forms (3.2), (3.3) and (3.4) can solve for the exact solution, when we choose $f(x) = x$ in (3.1) and $d = 1/2$, and if we take $S_h(\widehat{\Omega}) = P^3(\widehat{\Omega})$. The result is shown in Figure 2. It appears that all three formulations compute the exact solution. The computed Lagrange-multipliers for the hybrid- and Lagrange-formulation are shown in Table 1. We see that, in case of the hybrid-formulation, the Lagrange multipliers correspond with the fluxes at the boundaries, i.e., $p_h(0) = \frac{du}{dn}(0)$ and $p_h(1) = \frac{du}{dn}(1)$, whereas for the Lagrange-formulation, the Lagrange multipliers vanish.

Lagrange method	(3.2)	$p_h(d) = 0$	$p_h(1) = 0$
hybrid method	(3.3)	$p_h(0) = -5/25$	$p_h(1) = -7/24$

Table 1: The values of the Lagrange multipliers of hybrid- and Lagrange- method for the solution as in Figure 2.

Next we check if we can solve (2.2) for an arbitrary location $d \in [0, 1)$ of the interior Dirichlet boundary condition. Now we see that the dependencies on d and σ differ for the three methods. In case of the symmetric-/Baumann-Oden method we have to solve a full $(p+1) \times (p+1)$ linear system $L_{\sigma,d}\ u_h = f_h$, where the matrix depends on both the method parameter σ and the interior boundary location d.

In contrast, if we consider the coefficients of the linear system arising from the hybrid- and the Lagrange method we observe the following block-partitioning:

$$L_d\ u_h = \begin{pmatrix} \mathbf{A} & \mathbf{B} \\ \mathbf{C} & \mathbf{0} \end{pmatrix} u_h = f_h,$$

where, for the Lagrange method, $\mathbf{A} \cong \int_0^1 u_h' v_h' dx - [u_h'(1,0)v_h(1,0)]$ is the $(p+1) \times (p+1)$ leading submatrix, and $\mathbf{B} \cong [\overline{p}_h(d,1)v_h(d,1)]$ and $\mathbf{C} \cong [q_h(d,1)u_h(d,1)]$ have respectively dimensions $(p+1) \times 2$ and $2 \times (p+1)$. The dependency on d is reflected in the elements of $\mathbf{B}$ and $\mathbf{C}$.

On the other hand, in case of the hybrid-method, we have a $(p+1)\times(p+1)$ leading submatrix $\mathbf{A} \cong \int_0^1 u_h' v_h' dx$. Now the $(p+1)\times 2$ submatrix $\mathbf{B} \cong [p_h(0,1)v_h(0,1)]$ is independent of d. The dependency on d is only reflected in the $2\times(p+1)$ matrix $\mathbf{C} \cong [q_h(d,1)u_h(d,1)]$.

So we check if there are locations $d \in [0,1)$ in which any of the three methods may become singular. The results are shown in Table 2. We see that both the Lagrange- and the symmetric-/Baumann-method have interior boundary locations where the methods become singular. The number of points where a singularity appears increases with the polynomial degree. The hybrid-method, however, shows no singular points. This motivates us to continue mainly with the hybrid method for the two-dimensional numerical experiments.

The Lagrange method			
$p=2$	$1/3$	$-$	$-$
$p=3$	$2/5-1/10\sqrt{6}$	$2/5+1/10\sqrt{6}$	$-$
$p=4$	0.08858795951	0.4094668644	0.7876594618

The symmetric- / Baumann-method		
$p=2$	$-$	$-$
$p=3$	$2/5$	$-$
$p=4$	$3/7-1/7\sqrt{2}$	$3/7+1/7\sqrt{2}$

Table 2: Values of d for which the discrete system becomes singular. The discretisations are made for $S_h(\widehat{\Omega}) = P^p(0,1)$, $p=2,3,4$.

3.2 Numerical experiments for the hybrid-method on two-dimensional problems

Having studied the one-dimensional discretisation for the various weak formulations with an embedded Dirichlet boundary condition, we now consider the two-dimensional Poisson equation on the unit square $\widehat{\Omega}$ as in (2.2) with an embedded Dirichlet boundary condition on a line parallel to a diagonal. For this line we use the following parametrisation (See Figure 3):

$$\begin{cases} x(s) = 1 - d/\sqrt{2} + s, \\ y(s) = 1 - d/\sqrt{2} - s, \end{cases} \quad \text{with} \quad \begin{cases} |s| < d/\sqrt{2} & \text{if } 0 \le d \le 1/\sqrt{2}, \\ |s| < 1 - d/\sqrt{2} & \text{if } 1/\sqrt{2} < d < \sqrt{2}. \end{cases} \tag{3.5}$$

Approximation with piecewise quadratics. To discretize the hybrid formulation, we first introduce the quadratic polynomial basis on the unit interval

$$P^2([0,1]) = \text{Span}\{1-t,\ t,\ t(1-t)\}. \tag{3.6}$$

We provide the test and trial function spaces with the 9 dimensional subspace $S_h(\widehat{\Omega}) = P^{2\times 2}(\widehat{\Omega}) = P^2(x)\otimes P^2(y) \subset H^1(\widehat{\Omega})$, i.e., the tensor product set of polynomials of degree ≤ 2 in the two coordinate directions. Since we know that the Lagrange multiplier of the hybrid-method corresponds with the flux $p = \mathbf{n}\cdot\nabla u$ on the boundary $\partial\widehat{\Omega}$, we choose to discretize the Lagrange multiplier as $p_h = n_x\psi_x(x,y)|_{\partial\widehat{\Omega}} + n_y\psi_y(x,y)|_{\partial\widehat{\Omega}}$, with $\psi \in P^{2\times 2}(\widehat{\Omega})$ which defines the polynomial subspace $Q_h(\partial\widehat{\Omega}) \subset H^{-1/2}(\partial\widehat{\Omega})$ and also $Q_h(\partial\Omega) \subset H^{-1/2}(\partial\Omega)$

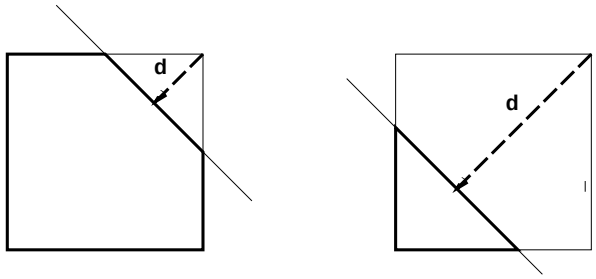

Figure 3: The domain Ω and its parametrisation

by $p_h|_{\partial\Omega} = n_x\psi_x(x,y)|_{\partial\Omega} + n_y\psi_y(x,y)_{\partial\Omega}$. Then the discrete formulation of the hybrid form is: find $u_h \in S_h(\widehat{\Omega})$, $p_h \in Q_h(\partial\widehat{\Omega})$ such that

$$\begin{aligned} \langle \nabla u_h, \nabla v_h \rangle_{S_h(\widehat{\Omega})} - \langle p_h, v_h \rangle_{Q_h(\partial\widehat{\Omega})} &= \langle f, v_h \rangle_{S_h(\widehat{\Omega})}, \quad \forall v_h \in S_h(\widehat{\Omega}), \\ \langle q_h, u_h \rangle_{Q_h(\partial\Omega)} &= \langle q, u_0 \rangle_{Q_h(\partial\Omega)}, \quad \forall q \in Q_h(\partial\Omega), \end{aligned} \tag{3.7}$$

where the approximations are given by (9 degrees of freedom describe the polynomial in the interior)

$$u_h(x,y) = \sum_{0\le i\le 8} c_i\phi_i(x,y), \qquad \phi_i \in S_h(\widehat{\Omega}), \qquad (x,y) \in \widehat{\Omega}, \tag{3.8}$$

and (notice that 8 degrees of freedom describe the quadratic polynomials at the 4 boundaries)

$$\begin{aligned} p_h(x,y) = \sum_{0\le i\le 7} a_i \left[n_x\psi_{x,i}(x,y)|_{\partial\widehat{\Omega}} + n_y\psi_{y,i}(x,y)|_{\partial\widehat{\Omega}} \right], \\ \psi_{x,i}|_{\partial\widehat{\Omega}}, \psi_{y,i}|_{\partial\widehat{\Omega}} \in Q_h(\partial\widehat{\Omega}), \qquad (x,y) \in \partial\widehat{\Omega}. \end{aligned} \tag{3.9}$$

The result is a 17×17 linear system depending on the diagonal distance of the embedded Dirichlet boundary to the origin. It is obvious that all methods will become ill-conditioned for values of d close to $\sqrt{2}$, when the region Ω vanishes. In order to see how the singularity develops for the *hybrid* method (2.7), we plot the 17 singular values as function of the diagonal distance d. The result is shown in Figure 4. We see that, as in the one-dimensional experiment, also for this experiment, there are no values of d for which the discretisation matrix becomes singular. Furthermore the method is not ill-conditioned for values of d even larger than one.

Approximation with piecewise cubics. Next we want to study the stability of a higher order discretisation of the hybrid method (2.7), for the same two-dimensional model problem. For that we consider on the unit interval the cubic polynomial basis

$$P^3([0,1]) = \{1-t,\ t,\ t(1-t)^2, t^2(1-t)\ \}, \tag{3.10}$$

and we choose for the test- and trial function spaces the 16-dimensional subspace $S_h(\widehat{\Omega}) = P^{3\times 3}(\widehat{\Omega}) = P^3(x) \otimes P^3(y) \subset H^1(\widehat{\Omega})$, i.e., the tensor product polynomials of degree less

than four in the two coordinate directions. We choose the polynomial subspaces $Q_h(\partial\widehat{\Omega}) = \gamma_1^{\partial\widehat{\Omega}}(S_h(\widehat{\Omega})) \subset H^{-1/2}(\partial\widehat{\Omega})$ and $Q_h(\partial\Omega) = \gamma_1^{\partial\Omega}(S_h(\widehat{\Omega})) \subset H^{-1/2}(\partial\Omega)$. The choice of the basis functions in $Q_h(\partial\Omega)$ will be explained in the next section, where we study the general case with a curved boundary.

As explained in Section 4, using (3.7) and (3.8) we obtain a 28×28 system depending on the diagonal distance d of the interior Dirichlet boundary to the origin. For this hybrid discretisation, the 28 singular values as function of d are shown in Figure 5. Generally, we observe the same behavior as for the quadratic polynomials.

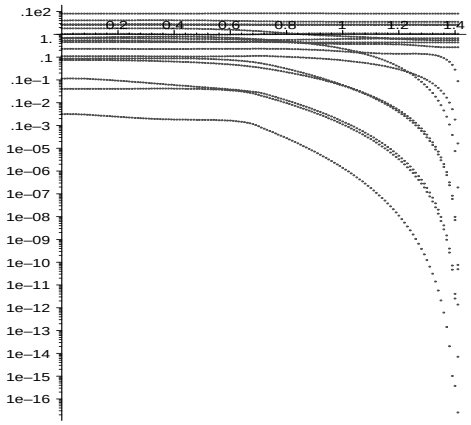

Figure 4: Singular values σ_i, $1 \leq i \leq 17$ as function of the diagonal distance $0 \leq d < \sqrt{2}$ for the third order discretisation of the hybrid method.

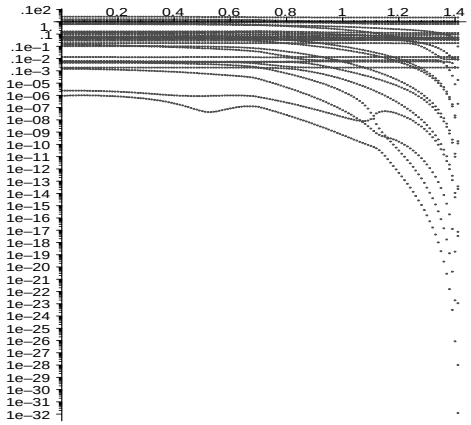

Figure 5: Singular values σ_i, $1 \leq i \leq 28$ as function of the diagonal distance $0 \leq d < \sqrt{2}$ for the fourth order discretisation of the hybrid method.

4. Weak forms for embedded boundary conditions

4.1 The boundary condition on a curved embedded boundary

In this section we study the stability and the accuracy of a fourth order hybrid discretisation of the Poisson equation on the unit square, with a part of the circular boundary embedded.

So, we solve the equation

$$-\Delta u = f \ \text{ on } \ \widehat{\Omega}, \qquad \text{with} \quad u = u_0 \ \text{ on } \ \Gamma_D = \partial\Omega, \tag{4.1}$$

on the unit square from which a circle sector has been removed: i.e., $\widehat{\Omega}$ the unit square and $\Gamma_{\text{int}} \subset \partial\Omega$, with $\Omega \subset \widehat{\Omega}$, is the circular curve

$$\Gamma_{\text{int}} = \left\{(x,y) \mid x^2 + y^2 = R^2 < 1,\ x \geq 0,\ y \geq 0\right\}, \tag{4.2}$$

and the fictitious part is

$$\widetilde{\Omega} = \left\{(x,y) \mid x > 0, y > 0, x^2 + y^2 < R^2\right\}. \tag{4.3}$$

The corresponding discrete hybrid formulation reads: find $u_h \in S_h(\widehat{\Omega})$, $\chi_h \in \ Q_h(\widehat{\Omega})$ such that

$$\begin{aligned} &(\nabla u_h, \nabla v_h)_{\widehat{\Omega}} - \left\langle \gamma_1^{\widehat{\Omega}}(\chi_h), \gamma_0^{\widehat{\Omega}}(v_h) \right\rangle_{\partial\widehat{\Omega}} = (f, v_h)_{\widehat{\Omega}}\,, && \forall v_h \in S_h(\widehat{\Omega}), \\ &\left\langle \gamma_1^{\Omega}(q_h), \gamma_0^{\Omega}(u_h) \right\rangle_{\partial\Omega} = \left\langle \gamma_1^{\Omega}(q_h), u_0 \right\rangle_{\partial\Omega}\,, && \forall q_h \in \ Q_h(\widehat{\Omega}), \end{aligned} \tag{4.4}$$

where $S_h(\widehat{\Omega}) \subset H^1(\widehat{\Omega})$ and $\ Q_h(\widehat{\Omega}) \subset H^1(\widehat{\Omega})$ are proper finite dimensional polynomial subspaces, and γ_0^{Ω}, γ_1^{Ω} and $\gamma_0^{\widehat{\Omega}}$, $\gamma_1^{\widehat{\Omega}}$ are the usual trace operators on $\partial\Omega$ and $\partial\widehat{\Omega}$ respectively. To provide these subspaces with a basis, we choose cubic polynomials and consider the following polynomial basis on the unit interval:

$$\begin{aligned} \phi_1 &= 1 - t, \qquad \phi_2 = (1-t)^2 t, \\ \phi_4 &= t, \qquad \phi_3 = (1-t)t^2. \end{aligned} \tag{4.5}$$

We recognize that $\phi_1(t)$ and $\phi_4(t)$ are associated with function values at $t = 0, 1$ respectively, while $\phi_2(t)$ and $\phi_3(t)$ can be associated with corrections for the derivatives at $t = 0, 1$. These facts help us to understand the structure behind the different polynomial subspaces that are constructed below.

First we choose for the test and trial function spaces the 16-dimensional subspace, i.e., $S_h(\widehat{\Omega}) = P^{3\times 3}(\widehat{\Omega}) = P^3(x) \otimes P^3(y) \subset H^1(\widehat{\Omega})$, the usual tensor product of polynomials of degree less than four in the two coordinate directions. Hence, on the unit square $\widehat{\Omega}$ we get the approximation $u_h \in S_h(\widehat{\Omega})$,

$$u_h = \sum_{1 \leq i,j \leq 4} c_{i,j} \phi_i(y) \phi_j(x)\,. \tag{4.6}$$

Next we consider the usual trace operators, $\gamma_0^{\widehat{\Omega}} : H^1(\widehat{\Omega}) \to H^{1/2}(\partial\widehat{\Omega})$ and $\gamma_0^{\Omega} : H^1(\widehat{\Omega}) \to H^{1/2}(\partial\Omega)$ applied to the boundary of $\widehat{\Omega}$ and Ω respectively, and similarly $\gamma_1^{\widehat{\Omega}} : H^1(\widehat{\Omega}) \to H^{-1/2}(\partial\widehat{\Omega})$ and $\gamma_1^{\Omega} : H^1(\widehat{\Omega}) \to H^{-1/2}(\partial\Omega)$ the traces for the normal derivatives. We see that the approximating space of tensor product cubics, $S_h(\widehat{\Omega}) \subset H^1(\widehat{\Omega})$, is a 16-dimensional subspace. The trace of this space on $\partial\widehat{\Omega}$, the space $\gamma_0^{\widehat{\Omega}}(S_h(\widehat{\Omega}))$, however, is 12-dimensional, because the trace consists of independent cubics on the four edges, related by four continuity conditions at the vertices. By the choice of the polynomial basis (4.5), in $S_h(\widehat{\Omega})$ a basis for

$\gamma_0^{\widehat{\Omega}}(S_h(\widehat{\Omega}))$ can readily be found as a subset of the tensor product of basis functions (4.5), by splitting $S_h(\widehat{\Omega})$ in two linearly independent subspaces:

$$S_h(\widehat{\Omega}) = \widetilde{Q}_h(\widehat{\Omega}) \oplus \widetilde{K}_h(\widehat{\Omega}) \,,$$

with

$$\widetilde{K}_h(\widehat{\Omega}) = \ker(\gamma_0^{\widehat{\Omega}}) \cap S_h(\widehat{\Omega}) = \text{Span}\left(\ \phi_i(x)\phi_j(y) \mid i,j = 2,3 \ \right) \,, \tag{4.7}$$

and

$$\widetilde{Q}_h(\widehat{\Omega}) = \text{Span}\left(\phi_1(x)\phi_j(y),\ \phi_4(x)\phi_j(y),\ \phi_i(x)\phi_1(y),\ \phi_i(x)\phi_4(y);\ i,j = 1,2,3,4\right). \tag{4.8}$$

For the approximating space for $\gamma_0^{\widehat{\Omega}}(H^1(\widehat{\Omega}))$ we take

$$Q_h^*(\partial\widehat{\Omega}) := \gamma_0^{\widehat{\Omega}}(S_h(\widehat{\Omega})) = \gamma_0^{\widehat{\Omega}}(\widetilde{Q}_h(\widehat{\Omega})) \subset H^{1/2}(\partial\widehat{\Omega}) \,.$$

Similarly we introduce the approximation space for the traces on $\partial\Omega$ as

$$Q_h^*(\partial\Omega) := \gamma_0^{\Omega}(\widetilde{Q}_h(\widehat{\Omega})) \subset H^{1/2}(\partial\Omega) \,.$$

On the other hand, for the approximation of the trace of the normal derivatives we split the space $S_h(\widehat{\Omega})$ as

$$S_h(\widehat{\Omega}) = \ Q_h(\widehat{\Omega}) \oplus K_h(\widehat{\Omega})$$

with

$$K_h(\widehat{\Omega}) = \ker(\gamma_1^{\widehat{\Omega}}) \cap S_h(\widehat{\Omega}) = \text{Span}\left(\ \psi_i(x)\psi_j(y) \mid i,j = 1,4 \ \right) \quad \text{with } \psi_k = \phi_k + (-)^k(\phi_3 - \phi_2),$$

and

$$Q_h(\widehat{\Omega}) = \text{Span}\left(\phi_2(x)\phi_j(y),\ \phi_3(x)\phi_j(y),\ \phi_i(x)\phi_2(y),\ \phi_i(x)\phi_3(y),\ i,j = 1,2,3,4\right) .$$

We see that $Q_h(\widehat{\Omega})$ is 12-dimensional and $K_h(\widehat{\Omega})$ is 4-dimensional. The normal derivatives on the four edges of $\widehat{\Omega}$ are all approximated by cubic polynomials that are related by the condition that at the vertices $\frac{1}{\partial x}(\frac{\partial u_h}{\partial y}) = \frac{1}{\partial y}(\frac{\partial u_h}{\partial x})$. So we find the approximating space for the normal derivatives at the boundary of $\widehat{\Omega}$, viz.,

$$Q_h(\partial\widehat{\Omega}) := \gamma_1^{\widehat{\Omega}}(S_h(\widehat{\Omega})) = \gamma_1^{\widehat{\Omega}}(\ Q_h(\widehat{\Omega})) \subset H^{-1/2}(\partial\widehat{\Omega})$$

and at the boundary of Ω as

$$Q_h(\partial\Omega) := \gamma_1^{\Omega}(\ Q_h(\widehat{\Omega})) \subset H^{-1/2}(\partial\Omega) \,.$$

Considering the Lagrange multiplier function $p \in H^{-1/2}(\partial\widehat{\Omega})$ in (2.7), we know that, if u satisfies Poisson's equation (4.1) and also the Dirichlet boundary condition, the Lagrange multiplier p on $\partial\widehat{\Omega}$ represents the normal flux $\mathbf{n}\cdot\nabla u$ at the the boundary $\partial\widehat{\Omega}$, i.e., $p = \mathbf{n}\cdot\nabla u$. So, in the discrete hybrid formulation (4.4), we write for the Lagrange multiplier $p_h = \mathbf{n}\cdot\nabla\chi_h$

on $\partial\widehat{\Omega}$, where n is the unit outward normal vector and $\chi_h \in Q_h(\widehat{\Omega})$ is the master flux function given by

$$\chi_h = \sum_{1\le i,j\le 4} a_{i,j}\phi_i(x)\phi_j(y), \qquad \text{with} \quad a_{i,j} = 0, \quad i,j = 1,4\,. \tag{4.9}$$

So we recognize the discrete hybrid formulation (4.4): find $u_h \in S_h(\widehat{\Omega})$, $\chi_h \in Q_h(\widehat{\Omega})$ such that

$$\begin{aligned} &(\nabla u_h, \nabla v_h)_{\widehat{\Omega}} - \left\langle \gamma_1^{\widehat{\Omega}}(\chi_h), \gamma_0^{\widehat{\Omega}}(v_h)\right\rangle_{\partial\widehat{\Omega}} = (f, v_h)_{\widehat{\Omega}}, && \forall v_h \in S_h(\widehat{\Omega}), \\ &\left\langle \gamma_1^{\Omega}(q_h), \gamma_0^{\Omega}(u_h)\right\rangle_{\partial\Omega} = \left\langle \gamma_1^{\Omega}(q_h), u_0\right\rangle_{\partial\Omega}\,, && \forall q_h \in Q_h(\widehat{\Omega}), \end{aligned} \tag{4.10}$$

as a $(16+12)\times(16+12)$ linear system. To study the stability of this hybrid formulation we plot the singular values of the discrete 28×28 system as function of the circle radius, $0 < R \le \sqrt{2}$. The result is shown in Figure 6. In this figure we see 28 singular values as a function of the circle radius, R. The discrete formulation is sufficiently stable up to circle radii of $R \approx 1.1$. In that case more than 80% of the total domain $\widehat{\Omega}$ consists of the fictitious domain $\widetilde{\Omega}$. A reason for the cusps in the figure near $R = 0.4$ and $R = 0.9$ is unknown.

Next, we check how the cubic approximation will solve for the exact solution by taking in (4.1) the right-hand side and the boundary conditions such that the solution is given by $u = x^3+y^3+xy$. The solution and the error for two possible domains ($R = 2/5$ and $R = 4/5$) are shown in the Figures 7 and 8. We see that the hybrid formulation finds the exact solution on the domain Ω, except for rounding errors which correspond with the condition of the linear system.

To check the approximation behavior of the method we repeat the experiment for the solution $u(x,y) = e^{x+y}$ in (4.1). The solution and the error for both domains ($R = 2/5$ and $R = 4/5$) are shown in the Figures 9 and 10.

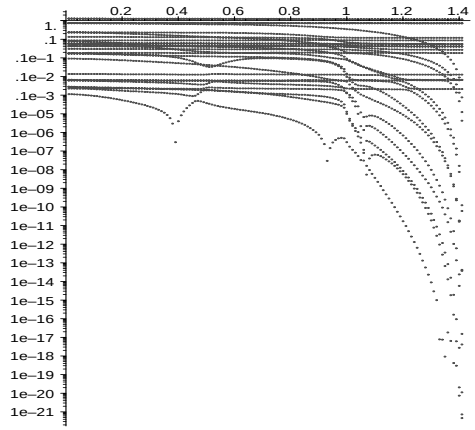

Figure 6: The singular values as function of the embedded circle bow radius for the fourth order hybrid discretisation. On the fictitious part of the domain the solution and the error are set equal to zero.

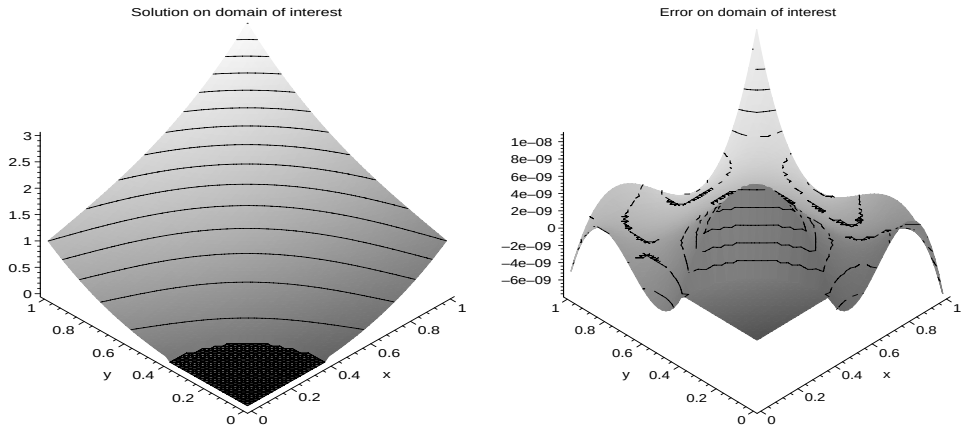

Figure 7: The solution $u = x^3 + y^3 + xy$ and the error on the domain Ω of the fourth order hybrid discretisation ($R = 2/5$).

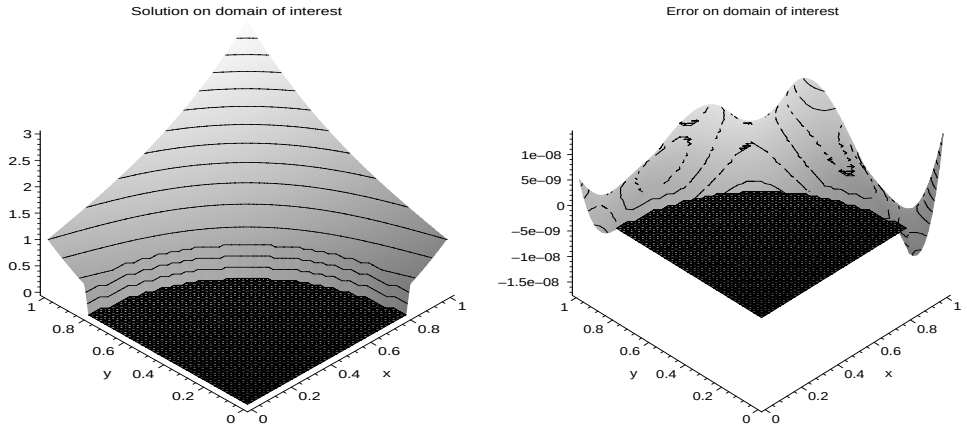

Figure 8: The solution $u = x^3 + y^3 + xy$ and the error on the domain Ω of the fourth order hybrid discretisation ($R = 4/5$).

4.2 The combination of the hybrid and the discontinuous Galerkin formulation

In the previous sections we have seen that the hybrid form is stable on a cell with an embedded Dirichlet boundary condition, whereas the discontinuous Galerkin method is not always stable. On the other hand the discontinuous Galerkin method is cheaper, because the Lagrange multiplier has been eliminated and hence less degrees of freedom are involved. So, to cut down on computational costs, if we consider a large regular rectangular grid on which locally there exist cells with embedded Dirichlet boundary conditions, it is natural to treat these cells with the hybrid method for stability, while the 'normal' rectangular cells are treated with a DG-Galerkin discretisation.

To study such a method, we consider two adjacent rectangular cells $\widehat{\Omega}_1$ and $\widehat{\Omega}_2$, where only $\widehat{\Omega}_1$ has an embedded Dirichlet boundary condition. The cells have a common interface $\Gamma_{1,2}$. Because cell $\widehat{\Omega}_1$ has an embedded boundary condition, we treat this cell with a hybrid

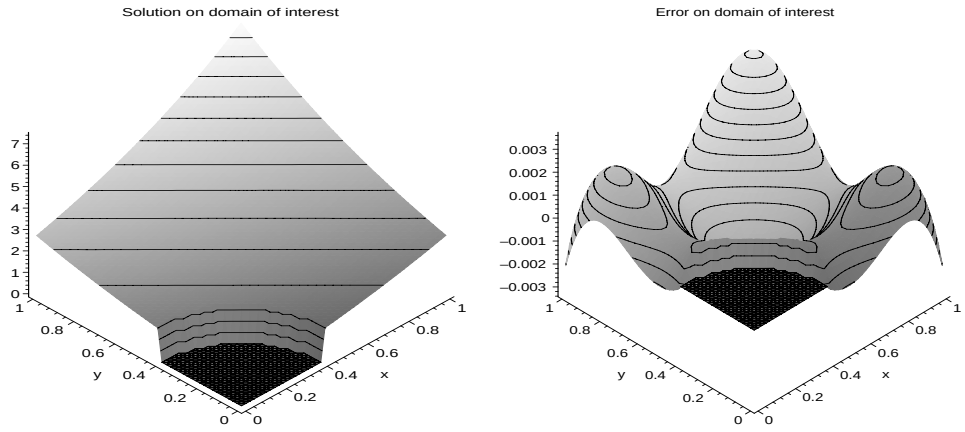

Figure 9: The solution $u = e^{x+y}$ and the error on the domain Ω of the fourth order hybrid discretisation ($R = 2/5$).

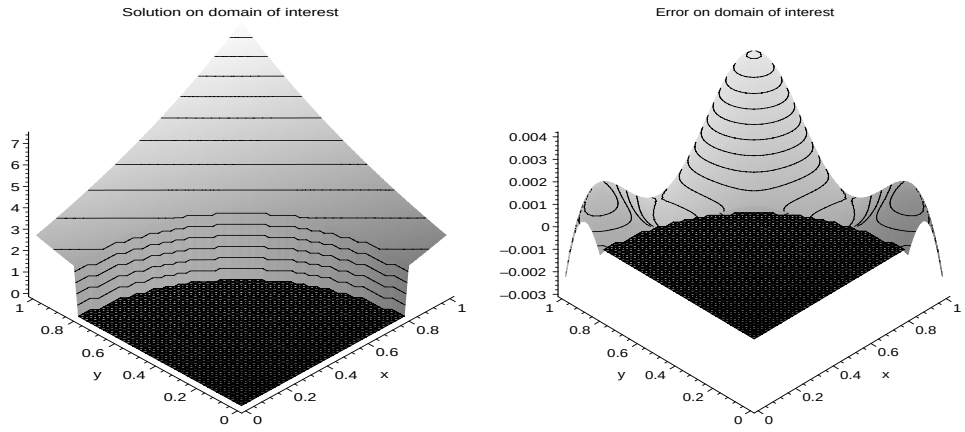

Figure 10: The solution $u = e^{x+y}$ and the error on the domain Ω of the fourth order hybrid discretisation ($R = 4/5$).

discretisation. Cell $\widehat{\Omega}_2$ is discretized by DG discretisation. So, on cell $\widehat{\Omega}_1$ we have

$$\begin{aligned}\int_{\widehat{\Omega}_1} \nabla u_h \cdot \nabla u_h dx - \int_{\Gamma_{1,2}} (\mathbf{n}_{1,2} \cdot \nabla \chi_h) v_h ds - \int_{\partial\widehat{\Omega}_1 \setminus \Gamma_{1,2}} (\mathbf{n} \cdot \nabla \chi_h) v_h ds \\ - \int_{\Gamma_{1,2}} (\mathbf{n}_{1,2} \cdot \nabla q_h) u_h ds - \int_{\partial\Omega_1 \setminus \Gamma_{1,2}} (\mathbf{n} \cdot \nabla q_h) u_h ds \\ = \int_{\widehat{\Omega}_1} f v_h dx - \int_{\partial\Omega_1 \setminus \Gamma_{1,2}} \mathbf{n} \cdot \nabla q_h u_0 ds,\end{aligned} \tag{4.11}$$

where $\mathbf{n}$ is the unit normal on the interface $\Gamma_{1,2}$ pointing from cell $\widehat{\Omega}_1$ towards cell $\widehat{\Omega}_2$. On the

other hand, on cell $\widehat{\Omega}_2$ we consider (for simplicity) the symmetric DG discretisation. Hence

$$\begin{aligned}\int_{\widehat{\Omega}_2} \nabla u_h \cdot \nabla u_h dx - \int_{\Gamma_{1,2}} (\mathbf{n}\cdot\nabla u_h) v_h \, ds - \int_{\partial\widehat{\Omega}_2\setminus\Gamma_{1,2}} (\mathbf{n}\cdot\nabla u_h) v_h \, ds \\ - \int_{\Gamma_{2,1}} (\mathbf{n}\cdot\nabla v_h) u_h \, ds - \int_{\partial\widehat{\Omega}_2\setminus\Gamma_{1,2}} (\mathbf{n}\cdot\nabla v_h) u_h \, ds \\ = \int_{\widehat{\Omega}_2} f v dx - \int_{\partial\widehat{\Omega}_2\setminus\Gamma_{1,2}} (\mathbf{n}\cdot\nabla v_h) u_0 \, ds,\end{aligned} \tag{4.12}$$

Now we have to couple the two cells at the interface $\Gamma_{1,2}$. Therefore, we have to satisfy the locality, consistency and conservation conditions as discussed in [1]. To meet these conditions we define average fluxes across the interface by

$$\left\langle \widetilde{\nabla u_h} \right\rangle = \frac{1}{2}(\nabla\chi_h|_{\partial\widehat{\Omega}_1} + \nabla u_h|_{\partial\Omega_2}) \text{ and } \left\langle \widetilde{\nabla v_h} \right\rangle = \frac{1}{2}(\nabla q_h|_{\partial\widehat{\Omega}_1} + \nabla v_h|_{\partial\Omega_2}), \tag{4.13}$$

and jumps by

$$[u_h] = u_h|_{\partial\widehat{\Omega}_1}\mathbf{n}_{1,2} + u_h|_{\partial\widehat{\Omega}_2}\mathbf{n}_{2,1}. \tag{4.14}$$

Then combining (4.11) and (4.12), together with the flux and jump relations, we arrive at the form

$$\begin{aligned}\int_{\widehat{\Omega}_1\cup\widehat{\Omega}_2} \nabla u_h\cdot\nabla v_h dx \quad & - \int_{\Gamma_{1,2}} \left\langle \widetilde{\nabla u_h} \right\rangle \cdot [v_h] \, ds \quad - \int_{\Gamma_{1,2}} \left\langle \widetilde{\nabla v_h} \right\rangle \cdot [u_h] \, ds \\ & - \int_{\partial\widehat{\Omega}_1\setminus\Gamma_{1,2}} (\mathbf{n}\cdot\nabla\chi_h) v_h ds \quad - \int_{\partial\widehat{\Omega}_2\setminus\Gamma_{1,2}} (\mathbf{n}\cdot\nabla u_h) v_h ds \\ & - \int_{\partial\Omega_1\setminus\Gamma_{1,2}} (\mathbf{n}\cdot\nabla q_h) u_h ds \quad - \int_{\partial\widehat{\Omega}_2\setminus\Gamma_{1,2}} (\mathbf{n}\cdot\nabla v_h) u_h ds \\ = \int_{\widehat{\Omega}_1\cup\widehat{\Omega}_2} f v_h dx \quad & - \int_{\partial\Omega_1\setminus\Gamma_{1,2}} (\mathbf{n}\cdot\nabla q_h) u_0 ds \quad - \int_{\partial\widehat{\Omega}_2\setminus\Gamma_{1,2}} (\mathbf{n}\cdot\nabla v_h) u_0 ds.\end{aligned} \tag{4.15}$$

This weak form can immediately be used for discretisation as described above. The solution and the error of such a combined discretisation with cubic polynomials is shown in Figure 11.

4.3 An embedded boundary for the convection equation

Having studied the discretisation of the Poisson equation, we now consider the convection equation with an interior Dirichlet boundary condition

$$\mathbf{b}\cdot\nabla u = f \text{ in } \widehat{\Omega}, \qquad u = u_0 \text{ on } \partial\Omega_{\text{in}}, \tag{4.16}$$

where $\mathbf{b}$ is a constant vector denoting the direction of the convection and $\partial\Omega_{\text{in}}$ is the inflow boundary of Ω such that the boundary of Ω is $\partial\Omega = \partial\Omega_{\text{in}} \cup \partial\Omega_{\text{out}}$. The inflow and outflow boundaries are defined by $\mathbf{b}\cdot\mathbf{n} < 0$ on $\partial\Omega_{\text{in}}$ and $\mathbf{b}\cdot\mathbf{n} > 0$ on $\partial\Omega_{\text{out}}$, respectively. Considering the boundary of the whole domain $\partial\widehat{\Omega}$, we split also this boundary in an upwind and downwind boundary such that $\partial\widehat{\Omega} = \partial\widehat{\Omega}_{\text{in}} \cup \partial\widehat{\Omega}_{\text{out}}$. Then, according to the Lagrange multiplier theorem

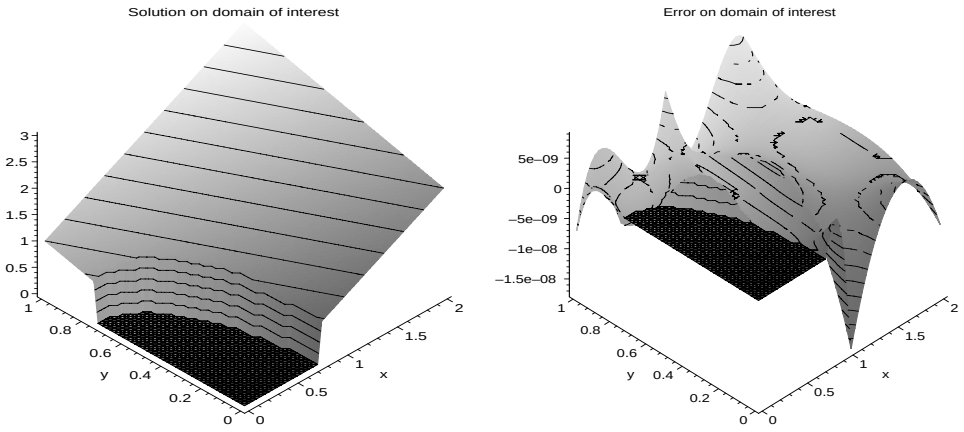

Figure 11: The approximate solution $u = x + y$ of $\Delta u = 0$, and the error on the domain $\Omega_1 \cup \widehat{\Omega}_2$ for a fourth order combined hybrid-symmetric DG discretisation with embedded circle segment Dirichlet boundary condition ($R = 3/4$).

we arrive for the boundary value problem at the following weak formulation:
find $u \in H^1(\widehat{\Omega})$ and $\chi \in H^{1/2}(\partial\widehat{\Omega}_{\text{in}})$ such that

$$\begin{aligned} &- \int_{\widehat{\Omega}} \nabla v \cdot \mathbf{b} u \; dx + \int_{\partial\widehat{\Omega}_{\text{in}}} \mathbf{n} \cdot \mathbf{b} \; \chi v \; ds + \int_{\partial\widehat{\Omega}_{\text{out}}} \mathbf{n} \cdot \mathbf{b} \; uv \; ds + \int_{\partial\Omega_{\text{in}}} \mathbf{n} \cdot \mathbf{b} \; qu \; ds \qquad (4.17) \\ &= \int_{\widehat{\Omega}} fv \; dx + \int_{\partial\Omega_{\text{in}}} \mathbf{n} \cdot \mathbf{b} \; qu_0 \; ds, \qquad \forall v \in H^1(\widehat{\Omega}), \; \forall q \in H^{1/2}(\partial\Omega_{\text{in}}), \end{aligned}$$

in which we assume that u on the fictitious domain $\widetilde{\Omega}$ satisfies the differential equation and is the continuation of the solution u on the domain Ω. Figure 12 shows the solution and the error if (4.17) is used as the starting point for a discretisation with cubic polynomials, as discussed above.

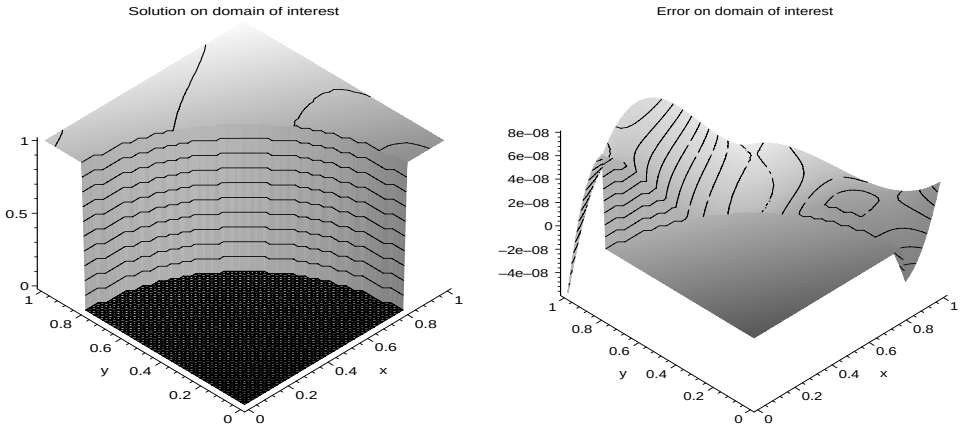

Figure 12: The approximate solution $u = 1$ of the convection equation $\mathbf{b} \cdot \nabla u = 0$ and the error on the domain Ω for a fourth order hybrid discretisation with embedded circle segment Dirichlet boundary condition ($R = 8/10$).

4.4 Two adjacent cells with a common interior embedded boundary condition
In this section we study a finite element discretisation of the convection diffusion equation

$$-\varepsilon\Delta u + \mathbf{b}\cdot\nabla u = 0\,, \tag{4.18}$$

discretized on two adjacent cells $\widehat{\Omega}_1$ and $\widehat{\Omega}_2$, with vertices $(-1,0),(0,0),(0,1),(-1,1)$ and $(0,0),(1,0),(1,1),(0,1)$ respectively. The embedded Dirichlet boundary condition is given on the half circle $x^2+y^2=R^2$, $0\le y\le 1$, so that the domain of interest is given by

$$\Omega = (\widehat{\Omega}_1\cup\widehat{\Omega}_2)\setminus\left\{(x,y)\mid x^2+y^2\ge R^2\right\}.$$

We first consider the diffusion part of the equation. Then, the weak hybrid formulation of the problem reads: find $u\in H^1(\widehat{\Omega}_h)$ and $p\in H^{-1/2}(\partial\widehat{\Omega}\cup\widehat{\Gamma}_{\text{int}})$ such that:

$$\begin{aligned}&(\nabla u,\nabla v)_{\widehat{\Omega}_h} - \langle p, v\rangle_{\partial\widehat{\Omega}} - \langle p,\mathbf{n}\cdot[v]\rangle_{\widehat{\Gamma}_{\text{int}}} - \langle q,u\rangle_{\partial\Omega} - \langle q,\mathbf{n}\cdot[u]\rangle_{\Gamma_{\text{int}}} \\ &= (f,v)_{\widehat{\Omega}_h} - \langle q,u_0\rangle_{\partial\Omega}\,, \qquad \forall v\in H^1(\widehat{\Omega}_h),\quad q\in H^{-1/2}(\partial\Omega\cup\Gamma_{\text{int}}),\end{aligned} \tag{4.19}$$

where $H^1(\widehat{\Omega}_h)$ is the broken Sobolev space on $\widehat{\Omega}_1\cup\widehat{\Omega}_2$ and the common interface is given by $\widehat{\Gamma}_{\text{int}}=\widehat{\Omega}_1\cap\widehat{\Omega}_2$, and $\mathbf{n}$ is the normal vector. The interface Γ_{int}, not including the fictitious part, is defined by $\Gamma_{\text{int}}=\overline{\Omega}_1\cap\overline{\Omega}_2$. Recognizing in $p|_{\widehat{\Gamma}_{\text{int}}}$ a normal flux on the common interface $\widehat{\Gamma}_{\text{int}}$, we define the trace operators, $\widetilde{\gamma}_1^{\widehat{\Omega}}: H^1(\widehat{\Omega})\cap C^1(\widehat{\Omega}) \to H^{-1/2}(\partial\widehat{\Omega}\cup\widehat{\Gamma}_{\text{int}})$ and $\widetilde{\gamma}_1^{\Omega}: H^1(\widehat{\Omega})\cap C^1(\widehat{\Omega}) \to H^{-1/2}(\partial\Omega\cup\Gamma_{\text{int}})$. In order to approximate the normal derivatives on $\partial\widehat{\Omega}\cup\widehat{\Gamma}_{\text{int}}$ we proceed as in Section 4.1 and introduce the polynomial subspace $S_h(\widehat{\Omega})\subset H^1(\widehat{\Omega})\cap C^1(\widehat{\Omega})$. We split this space as:

$$S_h(\widehat{\Omega}) = Q_h(\widehat{\Omega})\oplus K_h(\widehat{\Omega}),$$

with

$$K_h(\widehat{\Omega}) = \ker(\widetilde{\gamma}_1^{\widehat{\Omega}})\cap S_h(\widehat{\Omega}).$$

Then the discrete version of (4.19) reads: find $u_h\in S_h(\widehat{\Omega}_h)$ and $\chi_h\in Q_h(\widehat{\Omega})$ such that

$$\begin{aligned}(\nabla u_h,\nabla v_h)_{\widehat{\Omega}_h} &- \left\langle\widetilde{\gamma}_1^{\widehat{\Omega}}(\chi_h),\gamma_0(v_h)\right\rangle_{\partial\widehat{\Omega}} - \left\langle\widetilde{\gamma}_1^{\widehat{\Omega}}(\chi_h),[v_h]\right\rangle_{\widehat{\Gamma}_{\text{int}}} \\ &- \left\langle\widetilde{\gamma}_1^{\Omega}(q_h),\gamma_0(u_h)\right\rangle_{\partial\Omega} - \left\langle\widetilde{\gamma}_1^{\Omega}(q_h),[u_h]\right\rangle_{\Gamma_{\text{int}}} \\ &= (f,v_h)_{\widehat{\Omega}_h} - \left\langle\widetilde{\gamma}_1^{\Omega}(q_h),u_0\right\rangle_{\partial\Omega} \qquad \forall v_h\in S_h(\widehat{\Omega}_h),\ q_h\in Q_h(\widehat{\Omega}).\end{aligned} \tag{4.20}$$

(Notice the polynomial spaces used!) For the polynomial space $S_h(\widehat{\Omega}_h)$ we can take the usual space of piecewise cubic polynomials in each coordinate direction on the partitioning $\widehat{\Omega}_1\cup\widehat{\Omega}_2$. On the other hand, it is not trivial to find a cubic polynomial space for $Q_h(\widehat{\Omega})\subset H^1(\widehat{\Omega})\cap C^1(\widehat{\Omega})$. As we do not want to make our discretisation unnecessary complicated and expensive, we eliminate the extra degrees of freedom for χ_h by identifying them with ∇u_h. Similarly, identifying q_h and $\sigma\nabla v_h$ on $\partial\Omega\cup\Gamma_{\text{int}}$ we arrive at a discontinuous Galerkin discretisation.

As our first interest is an efficient fourth order discretisation, we expect it to be highly improbable that instability will occur in the discrete operator, because the one-dimensional experiment shows only a single pole. Nevertheless, the use of DG discretisation forces us to monitor for possible singularities. Now the DG version of (4.20) is: find $u_h \in S_h(\widehat{\Omega}_h)$ such that

$$\begin{aligned}&(\nabla u_h, \nabla v_h)_{\widehat{\Omega}_h} - \langle \nabla u_h, v_h \rangle_{\partial\widehat{\Omega}} - \langle \langle \nabla u_h \rangle, [v_h] \rangle_{\widehat{\Gamma}_{\text{int}}} + \sigma \langle \nabla v_h, u_h \rangle_{\partial\Omega} + \\ &\sigma \langle \langle \nabla v_h \rangle, [u] \rangle_{\Gamma_{\text{int}}} = (f, v_h)_{\widehat{\Omega}_h} + \sigma \langle \langle \nabla v_h \rangle, u_0 \rangle_{\partial\Omega}, \qquad \forall v \in S_h(\widehat{\Omega}_h),\end{aligned} \tag{4.21}$$

with the usual choices for the normal flux functions.

Next we consider the convection part of (4.18). So, on the domain $\widehat{\Omega}$ we consider the equation

$$\mathbf{b} \cdot \nabla u = f, \qquad u = u_0 \text{ on } \partial\Omega_{\text{in}}. \tag{4.22}$$

For simplicity we set $\mathbf{b} = (1, 0)$. Then the embedded boundary is an outflow boundary for $\widehat{\Omega}_1$, whereas for $\widehat{\Omega}_2$ it is an inflow boundary. Hence, we can neglect this embedded boundary in $\widehat{\Omega}_1$, whereas in cell $\widehat{\Omega}_2$ we must introduce a Lagrange multiplier in order to satisfy the upwind boundary condition on the circle bow. Hence, we arrive at the following weak form for the convection part: find $u, \chi \in H^1(\widehat{\Omega}_h) = H^1(\widehat{\Omega}_1 \cup \widehat{\Omega}_2)$

$$\begin{aligned}-\int_{\widehat{\Omega}} \nabla v \cdot \mathbf{b} u dx &+ \int_{\partial\widehat{\Omega}_{1,\text{out}}} (\mathbf{n} \cdot \mathbf{b} u) v ds + \int_{\partial\widehat{\Omega}_{2,\text{in}}} (\mathbf{n} \cdot \mathbf{b}\chi) v ds + \int_{\partial\widehat{\Omega}_{2,\text{out}}} (\mathbf{n} \cdot \mathbf{b} u) v ds \\ &+ \int_{\partial\Gamma_{\text{int}}} (\mathbf{n} \cdot \mathbf{b} q) u ds - \int_{\Gamma_{\text{int}}} (\mathbf{n} \cdot \mathbf{b} q) u^- ds \\ = \int_{\widehat{\Omega}} f v dx &- \int_{\partial\widehat{\Omega}_{1,\text{in}}} (\mathbf{n} \cdot \mathbf{b} u_0) v ds + \int_{\Gamma_D} (\mathbf{n} \cdot \mathbf{b} q) u_0 ds \\ &\forall v, q \in H^1(\widehat{\Omega}),\end{aligned} \tag{4.23}$$

where $u^- = u|_{\partial\Omega_1} = u|_{\Gamma_{\text{int}}}$. If we want to eliminate in (4.23) the extra degrees of freedom, we set $\chi = u$ and $q = v$.

Linear combination of (4.21) and (4.23) gives a discretisation of the convection diffusion equation

$$-\Delta u + \mathbf{b} \cdot \nabla u = f \quad \text{ in } \widehat{\Omega}, \qquad u = u_0 \quad \text{ on } \partial\Omega. \tag{4.24}$$

The Figures 13 and 14 show the solution and the error of a discretisation of (4.24) by means of (4.21) and (4.23) with tensor-product cubics as approximation and test spaces.

5. A singularly perturbed PDE on only two cells with a half circle excluded

In this section we are interested to solve the following convection diffusion problem. (see Figure 15) More details about this problem can be found in [5]

$$-\varepsilon\Delta u + u_x = f \text{ on } \widehat{\Omega} = \{\, (x, y) \mid -1 < x < 1,\ 0 < y < 1 \}, \tag{5.1}$$

$$\begin{aligned}u &= 0 && \text{on } \partial\Omega = \{\, (x, y) \mid x = -1,\ 0 < y < 1;\ -1 < x < 1, y = 1 \}, \\ u &= 1 && \text{on } \Gamma_D = \{\, (x, y) \mid x^2 + y^2 = R^2, y > 0;\ R < 1 \}, \\ \mathbf{n} \cdot \varepsilon\nabla u &= 0 && \text{on } \Gamma_N = \{\, (x, 0) \mid R < |x| < 1 \} \cup \{\, (1, y) \mid 0 < y < 1 \}.\end{aligned} \tag{5.2}$$

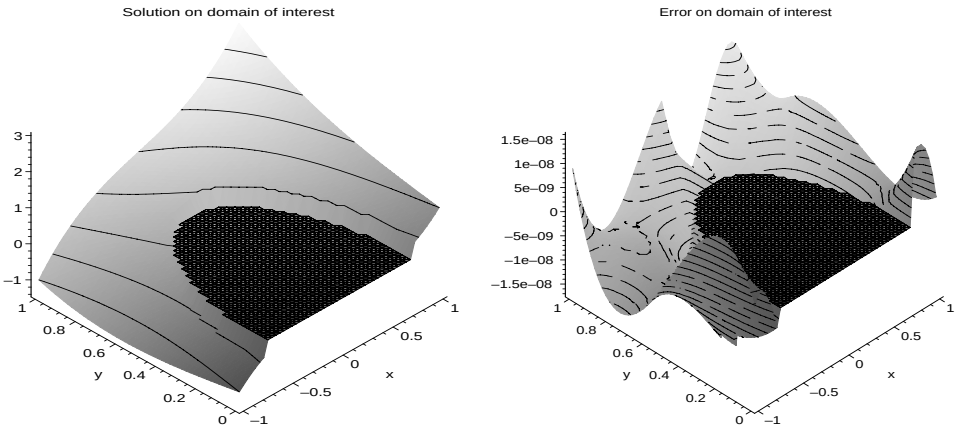

Figure 13: The approximate solution $u = x^3 + y^3 + xy$ of $-\Delta u + u_x = f$ and the error on the domain $\Omega = \Omega_1 \cup \Omega_2$ for a fourth order symmetric-DG discretisation with embedded circle Dirichlet boundary condition ($R = 3/4$).

Let $\widehat{\Omega}_1$ and $\widehat{\Omega}_2$ be two unit cells with respectively vertices $(-1,0),(0,0),(0,1),(-1,1)$ and $(0,0),(1,0),(1,1),(0,1)$ so that $\overline{\widehat{\Omega}} = \overline{\widehat{\Omega}}_1 \cup \overline{\widehat{\Omega}}_2$. For this problem we want to study the symmetric and the Baumann-Oden DG-method.

First we study the diffusion part of (5.1) and replace the homogeneous Neumann boundary condition on $\Gamma_N = \{\ (x,y) \mid x = 0,\ 0 < y < 1\}$ with the homogeneous Dirichlet boundary condition, in order to obtain a problem symmetric around $x = 0$. Now the corresponding *hybrid* formulation (2.7) for (5.1) reads: find $u \in H^1(\widehat{\Omega}_h)$ and $p \in H^{-1/2}(\partial\widehat{\Omega} \cup \widehat{\Gamma}_{\rm int})$ such that

$$\begin{aligned}(\nabla u, \nabla v)_{\widehat{\Omega}} - \langle p, v\rangle_{\partial\widehat{\Omega}} - \langle q, u\rangle_{\partial\Omega\cup\Gamma_D} - \langle p, \mathbf{n}\cdot[v]\rangle_{\widehat{\Gamma}_{\rm int}} - \langle q, \mathbf{n}\cdot[u]\rangle_{\Gamma_{\rm int}} = \\ = (f, v) - \langle q, u_0\rangle_{\partial\Omega\cup\Gamma_D}\,, \qquad \forall v \in H^1(\widehat{\Omega}_h),\ q \in H^{-1/2}(\partial\widehat{\Omega}\cup\Gamma_{\rm int}).\end{aligned} \tag{5.3}$$

Here $H^1(\widehat{\Omega}_h)$ is the broken Sobolev space on $\widehat{\Omega}_1 \cup \widehat{\Omega}_2$ and the jump operator is given by $[v] = \mathbf{n}_1 v|_{\partial\widehat{\Omega}_1} + \mathbf{n}_2 v|_{\partial\widehat{\Omega}_2}$. Further, $\Gamma_{\rm int} = \partial\Omega_1 \cap \partial\Omega_2$ is the interior wall on which the true solution is continuous. However, continuity is not required outside Ω and hence not on all of $\widetilde{\Gamma}_{\rm int} = \widehat{\Gamma}_{\rm int} \cap \widetilde{\Omega}$.

To arrive at the DG-discretisation of (5.3) we take for the test and trial space, $S_h(\widehat{\Omega}) \subset H^1(\widehat{\Omega}_h)$, the tensor product of polynomials of degree $p < 4$ in each of the coordinate directions and we write for the approximation

$$u_h = \sum_{0\le e<2}\ \sum_{0\le i,j<4} c_{e,i,j}\ \phi_{e,i}(x)\ \phi_{e,j}(y)\,. \tag{5.4}$$

In practice we construct a basis from (4.5).

Next, for the DG discretisation, we eliminate the extra equations and degrees of freedom for the Lagrange multiplier using the fact that p represents the normal flux of u at $\partial\widehat{\Omega}$ and at the internal wall $\widehat{\Gamma}_{\rm int}$. So replacing p by $\mathbf{n}\cdot\nabla u_h$ on $\partial\widehat{\Omega}$ and by $\langle \mathbf{n}\cdot\nabla u_h\rangle$ on $\widehat{\Gamma}_{\rm int}$ and replacing

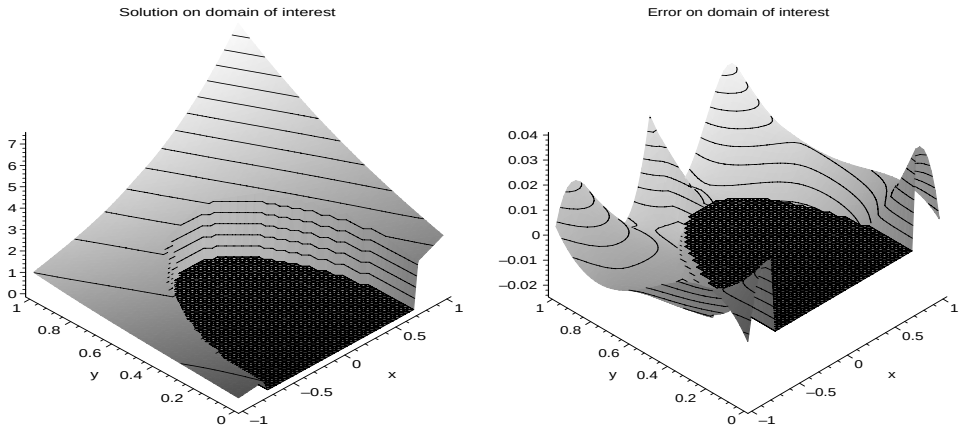

Figure 14: The approximate solution $u = e^{x+y}$ of $-\Delta u + u_x = f$ and the error on the domain $\Omega_1 \cup \Omega_2$ for a fourth order symmetric-DG discretisation with embedded circle Dirichlet boundary condition ($R = 3/4$).

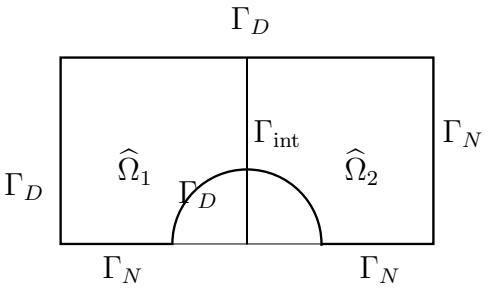

Figure 15: The domain for problem (5.1-5.2).

similarly q by $-\sigma \mathbf{n} \cdot \nabla v$, the DG discretisation of (5.3) reads: find $u_h \in S_h(\widehat{\Omega})$ such that

$$(\nabla u_h, \nabla v_h)_{\widehat{\Omega}} - \langle \mathbf{n} \cdot \nabla u_h, v_h \rangle_{\partial \widehat{\Omega}} + \sigma \langle \mathbf{n} \cdot \nabla v_h, u_h \rangle_{\partial \Omega \cup \Gamma_D} - \langle \langle \nabla u_h \rangle, [v] \rangle_{\widehat{\Gamma}_{\text{int}}} \tag{5.5}$$
$$+\sigma \langle \langle \nabla v_h \rangle, [u] \rangle_{\Gamma_{\text{int}}} = (f, v_h) + \sigma \langle \mathbf{n} \cdot \nabla v_h, u_0 \rangle_{\partial \Omega \cup \Gamma_D}, \qquad \forall v_h \in S_h(\widehat{\Omega}).$$

Figure 16 shows the solution of the symmetric ($\sigma = -1$) and Baumann-Oden ($\sigma = 1$) discretisation. We see that both solutions are symmetric indeed, because of the symmetric structure of the problem. On the other hand we recognize the instable behavior of the symmetric DG method, which is of poor quality compared with the solution of the Baumann-Oden method.

We continue by considering both methods for the diffusion part of the equation and boundary conditions as in (5.2). Then the discrete formulation is also given by (5.5), except that the Dirichlet boundary condition at $\{(1, y) \mid 0 < y < 1\}$ is replaced by the homogeneous Neumann boundary condition $\mathbf{n} \cdot \nabla u = 0$. The corresponding solutions of the symmetric and Baumann-Oden method are shown in Figure 17. Now the solutions are not symmetric. Again, the solution of the symmetric DG-method is poor compared to the solution of the Baumann-Oden DG method.

Finally, we take the convection part of (5.1). The Lagrange weak formulation of the

convection term for the cell $\widehat{\Omega}_2$ reads: find $u \in H^1(\widehat{\Omega}_2)$ and $\overline{p} \in H^{1/2}(\partial\Omega_{\text{in}})$ such that

$$\begin{aligned} -(\nabla v \cdot \mathbf{b}, u)_{\widehat{\Omega}_2} + \oint_{\partial\widehat{\Omega}_2} v\mathbf{n}\cdot\mathbf{b}u \; ds + \langle \overline{p}\;\mathbf{n}\cdot\mathbf{b}, v\rangle_{\partial\Omega_{\text{in}}} = 0,\ \forall v \in H^1(\widehat{\Omega}_2), \\ \langle q\mathbf{n}\cdot\mathbf{b}, u\rangle = \langle q\mathbf{n}\cdot\mathbf{b}, u_0\rangle\,,\ \forall q \in H^{1/2}(\partial\Omega_{\text{in}}), \end{aligned} \tag{5.6}$$

with $\mathbf{b} = (1,0)$ and $u_0 = 1$ on the embedded circle, $\Gamma_D \cap \partial\Omega_{\text{in}}$, while $u_0 = u^-$ on the common interior boundary, $\Gamma_{\text{int}} \cap \partial\Omega_{\text{in}}$, with u^- the upwind value of u obtained from $\widehat{\Omega}_1$.

As for the diffusion term, we can rewrite (5.6) in a *hybrid* formulation, where the Lagrange multiplier is computed on $\partial\widehat{\Omega}_{\text{in}}$, the inflow edge of the domain $\widehat{\Omega}_2$. Thus, we obtain: find $u \in H^1(\widehat{\Omega}_2)$ and $\widetilde{p} \in H^{1/2}(\partial\widehat{\Omega}_{\text{in}})$ such that

$$\begin{aligned} -(\nabla v \cdot \mathbf{b}, u)_{\widehat{\Omega}_2} + \oint_{\partial\widehat{\Omega}_2} v\mathbf{n}\cdot\mathbf{b}u \; ds + \langle \widetilde{p}\;\mathbf{n}\cdot\mathbf{b}, v\rangle_{\partial\widehat{\Omega}_{\text{in}}} = 0, \qquad \forall v \in H^1(\widehat{\Omega}_2), \\ \langle q\mathbf{n}\cdot\mathbf{b}, u\rangle_{\partial\Omega_{\text{in}}} = \langle q\mathbf{n}\cdot\mathbf{b}, u_0\rangle_{\partial\Omega_{\text{in}}}\,, \qquad \forall q \in H^{1/2}(\partial\Omega_{\text{in}}). \end{aligned} \tag{5.7}$$

Next, the second term in (5.7) is split in an integration part over the inflow and a part over the outflow edge of $\partial\widehat{\Omega}_2$ so that we can combine the integration of u and $\widetilde{p}$ over the inflow wall $\partial\widehat{\Omega}_{\text{in}}$. This yields: find $u \in H^1(\widehat{\Omega}_2)$ and $p \in H^{1/2}(\partial\widehat{\Omega}_{\text{in}})$ such that

$$\begin{aligned} -(\nabla v \cdot \mathbf{b}, u)_{\widehat{\Omega}_2} + \langle(\widetilde{p}+u)\;\mathbf{n}\cdot\mathbf{b}, v\rangle_{\partial\widehat{\Omega}_{\text{in}}} + \langle u\;\mathbf{n}\cdot\mathbf{b}, v\rangle_{\partial\widehat{\Omega}_{\text{out}}} + \langle q\mathbf{n}\cdot\mathbf{b}, u\rangle_{\partial\Omega_{\text{in}}} \\ = \langle q\mathbf{n}\cdot\mathbf{b}, u_0\rangle_{\partial\Omega_{\text{in}}}\,, \qquad \forall v \in H^1(\widehat{\Omega}_2),\ \forall q \in H^{1/2}(\partial\Omega_{\text{in}}). \end{aligned} \tag{5.8}$$

Writing $p = \widetilde{p} + u$, this is simplified to: find $u \in H^1(\widehat{\Omega}_2)$ and $p \in H^{1/2}(\partial\widehat{\Omega}_{\text{in}})$ such that

$$\begin{aligned} -(\nabla v \cdot \mathbf{b}, u)_{\widehat{\Omega}_2} + \langle p\;\mathbf{n}\cdot\mathbf{b}, v\rangle_{\partial\widehat{\Omega}_{\text{in}}} + \langle u\;\mathbf{n}\cdot\mathbf{b}, v\rangle_{\partial\widehat{\Omega}_{\text{out}}} + \langle q\mathbf{n}\cdot\mathbf{b}, u\rangle_{\partial\Omega_{\text{in}}} \\ = \langle q\mathbf{n}\cdot\mathbf{b}, u_0\rangle_{\partial\Omega_{\text{in}}}\,, \qquad \forall v \in H^1(\widehat{\Omega}_2),\ \forall q \in H^{1/2}(\partial\Omega_{\text{in}}). \end{aligned} \tag{5.9}$$

To eliminate the Lagrange multiplier p, we recognize this function as the value of u at the boundary $\partial\widehat{\Omega}_{\text{in}}$. The corresponding equations are eliminated by taking $q = \sigma v$ on $\partial\Omega_{\text{in}}$, yielding the DG-formulation of the convection term: find $u \in H^1(\widehat{\Omega}_2)$ such that

$$\begin{aligned} -(\nabla v \cdot \mathbf{b}, u)_{\widehat{\Omega}_2} + \oint_{\partial\widehat{\Omega}_2} v\mathbf{n}\cdot\mathbf{b}u \; ds + \sigma\left\langle v\;\mathbf{n}\cdot\mathbf{b}, \left(u-u^-\right)\right\rangle_{\Gamma_{\text{int}}} \\ +\sigma\left\langle v\;\mathbf{n}\cdot\mathbf{b}, u\right\rangle_{\Gamma_D} = \sigma\left\langle v\;\mathbf{n}\cdot\mathbf{b}, u_0\right\rangle_{\Gamma_D}\,, \qquad \forall v \in H^1(\widehat{\Omega}_2). \end{aligned} \tag{5.10}$$

In cell Ω_1 the embedded boundary is an outflow boundary and, hence, for the convection part gives no boundary condition. Therefore, we may treat $\widehat{\Omega}_1$ as a normal convection DG-cell.

The discretisation of problem (5.1) is obtained by combining (5.5), (5.8), and (5.10): find $u_h \in S_h(\widehat{\Omega})$ such that

$$\begin{aligned} &(\varepsilon\nabla u_h, \nabla v_h)_{\widehat{\Omega}} - \langle \mathbf{n}\cdot\varepsilon\nabla u_h, v_h\rangle_{\partial\widehat{\Omega}} + \sigma\left\langle \mathbf{n}\cdot\varepsilon\nabla v_h, u_h\right\rangle_{\partial\Omega\cup\Gamma_D} - \left\langle\langle\varepsilon\nabla u_h\right\rangle, [v_h]\rangle_{\widehat{\Gamma}_{\text{int}}} \\ &+\sigma\left\langle\langle\varepsilon\nabla v_h, [u_h]\right\rangle\rangle_{\Gamma_{\text{int}}} - (\nabla v_h\cdot\mathbf{b}, u_h)_{\widehat{\Omega}} + \langle v_h\mathbf{n}\cdot\mathbf{b}, u_h\rangle_{\partial\widehat{\Omega}_{1,out}} + \oint_{\partial\widehat{\Omega}_2} v_h\mathbf{n}\cdot\mathbf{b}u_h \; ds \\ &+\sigma\left\langle v_h\mathbf{n}\cdot\mathbf{b}, \left(u_h-u_h^-\right)\right\rangle_{\Gamma_{\text{int}}} + \sigma\left\langle v_h\mathbf{n}\cdot\mathbf{b}, u_h\right\rangle_{\Gamma_D\cap\partial\Omega_2} \\ &=\sigma\left\langle \mathbf{n}\cdot\varepsilon\nabla v_h, 1\right\rangle_{\Gamma_D} + \sigma\left\langle v_h\mathbf{n}\cdot\mathbf{b}, 1\right\rangle_{\Gamma_D\cap\partial\Omega_2}\,, \qquad \forall v_h \in S_h(\widehat{\Omega}). \end{aligned} \tag{5.11}$$

Figure 18 shows the solutions of the fourth order discretisation of (5.11) for $R = 3/10$, for the different values of $\varepsilon = 1,\ 0.1,\ 0.02,\ 0.01$. We see that in all cases the solution is stable. For values of $\varepsilon = O(1)$ we see clearly the approximation of the boundary condition $u_0 = 1$ on the circle bow, while for small values of ε, when the true solution shows a thin boundary layer, typical effects of the weak boundary requirement show up. Figure 19 shows the solution for $\varepsilon = 1/50$. Although it seems that the solution is not capable to catch the boundary layer in Ω at the upwind side of the circle, we clearly see a boundary layer arise in the fictitious part of the domain if we consider the total $\widehat{\Omega}$. Clearly, the cubics are not able to represent the thin circular boundary layer. Notice in particular, at $x = 0$, $y < R$, the discontinuity in the fictitious part $\widetilde{\Omega}$. For small values of $\varepsilon << 1$ the boundary layer disappears.

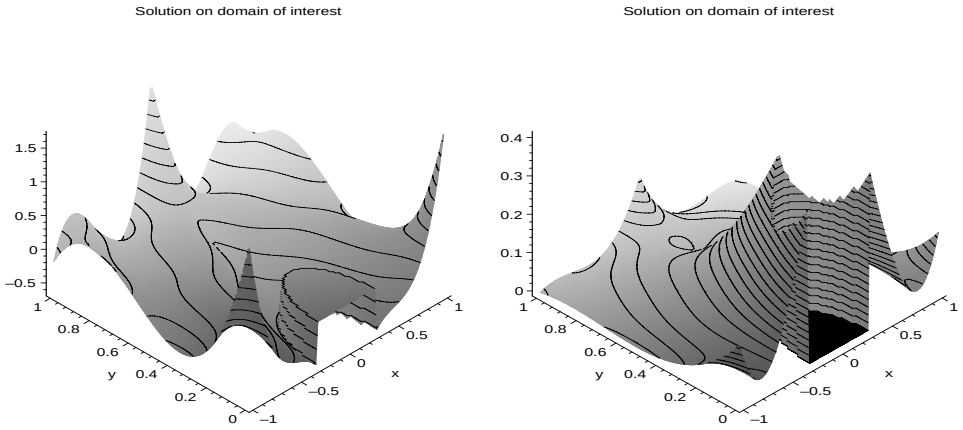

symmetric DG Baumann-Oden DG

Figure 16: The approximate solution u_h of $\Delta u = 0$ on the domain Ω with symmetric boundary conditions and fourth order discretisations with embedded circle Dirichlet boundary condition ($R = 3/10$).

6. Conclusion

In this paper we propose a technique for the treatment of second-order elliptic PDEs with complex Dirichlet boundary conditions in combination with discontinuous Galerkin discretisation. The aim is to maintain a structured, regular rectangular grid while solving problems with irregular curved boundary conditions.

The complex domain on which the solution is sought, is covered by a fictitious domain with the structured, regular rectangular grid. An embedded boundary is the transition between the domain of interest and the fictitious part of the computational domain.

We present and compare several weak forms for the diffusion part of the equation: the Lagrange multiplier form, the hybrid form and the DG-form. The hybrid form shows stability for an arbitrary location of the embedded boundary, whereas for the other forms the discretisation may become instable for particular locations of the Dirichlet BC. The problem is studied, first for a single cell and then for a couple of adjacent cells, either sharing or not sharing the embedded boundary. We also describe the treatment of a convection part in the equation.

As an example, we solve a singularly perturbed boundary value problem on a complex do-

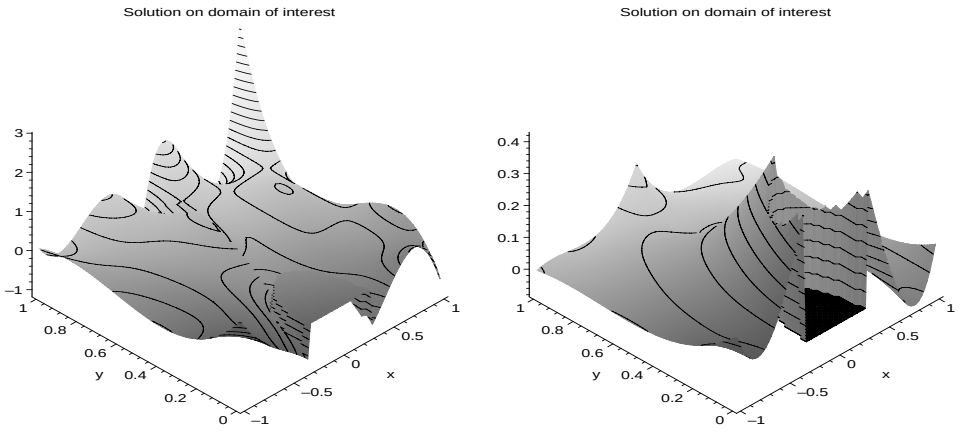

symmetric DG Baumann-Oden DG

Figure 17: The approximate solution u_h of $\Delta u = 0$ on the domain $\widehat{\Omega}$ with the boundary conditions (5.2) for a fourth-order symmetric and Baumann-Oden discontinuous Galerkin discretisation. The embedded circle Dirichlet boundary condition is located at $R = 3/10$.

main by means of a fourth-order DG-discretisation on only two cells. Although –as expected– it appears to be impossible to accurately represent sharp boundary layers with a complex structure by means of a few cubic polynomials, the boundary condition treatment is quite effective in handling such complex situations.

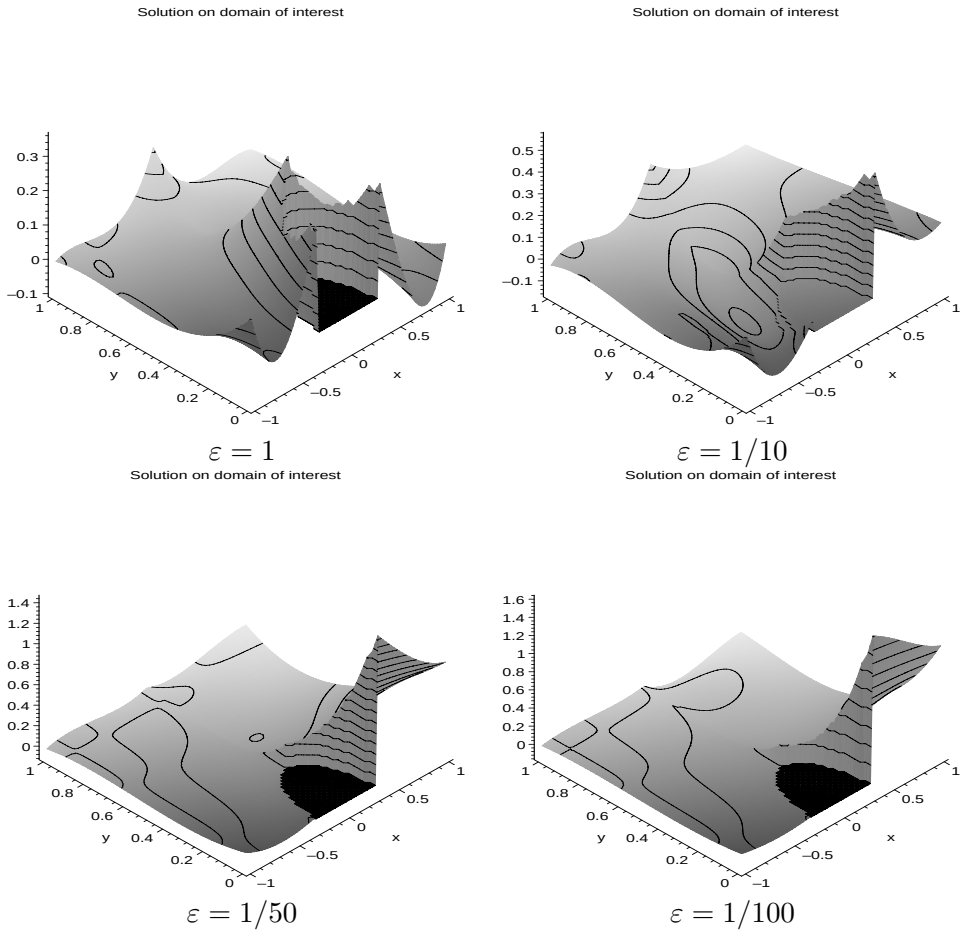

Figure 18: The approximate solution u_h of $-\varepsilon\Delta u + u_x = 0$, on the domain exterior of the circle for a fourth order Baumann-Oden DG discretisation with Dirichlet boundary condition $u_0 = 1$ on the circle, $(R = 3/10)$.

References

1. D.N. Arnold, F. Brezzi, B. Cockburn, and D. Marini. Unified analysis of discontinuous Galerkin methods for elliptic problems. *SIAM J Numer. Anal.*, pages 1749 – 1779, 2002.
2. R. Cortez and M. Minion. The Blob projection method for immersed boundary problems. *Journal of Computational Physics*, 161:428–453, 2000.
3. D. Goldstein, R. Handler, and L. Sirovich. Modeling a no-slip flow boundary with an external flow field. *J. Comp. Phys.*, 105:354–366, 1993.
4. W. Hackbusch. *Theorie und Numerik elliptischer Differentialgleichungen.* Teubner Studienbuecher, 1986.
5. P. W. Hemker. A singularly perturbed model problem for numerical computation. *Journal of Comp. and Appl. Math.*, 76:277–285, 1997.
6. P.W. Hemker, W. Hoffmann, and M.H. van Raalte. Two-level fourier analysis of a multigrid approach for discontinuous galerkin discretisation. Technical Report MAS-R0206,

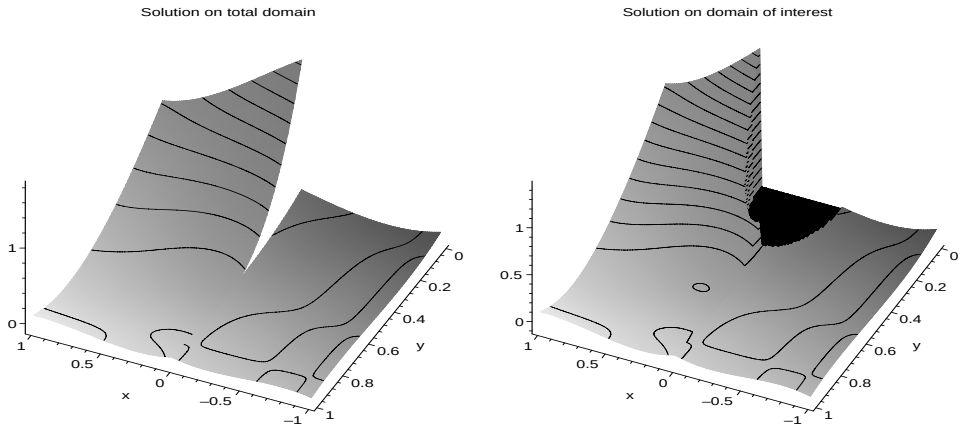

Total domain Domain of interest

Figure 19: The approximate solution u_h for the same problem as in Figure 18, with $\varepsilon = 1/50$. At the right, the approximate solution on Ω, the domain of interest. Left, the approximate solution on $\widehat{\Omega}$, the whole domain where the approximation is constructed, including the fictitious part.

CWI, Amsterdam, April 2002. submitted to SIAM SISC.

7. D. W. Hewett. The embedded curved boundary method for orthogonal simulation meshes. *J. Comp. Phys.*, 138:585 – 616, 1997.

8. D.W. Hewett and C.S. Kueny. The dielectric boundary condition for the embedded curved boundary (ECB) method. Technical Report UCRL-JC-129703, Lawrence Livermore Nat. Lab., 1998. presented at the 16th International Conference on the Numerical Simulation of Plasmas, February 1998, Santa Barbara, CA.

9. Jungwoo Kim, Dongjoo Kim, and Haecheon Choi. An immersed-boundary finite-volume method for simulations of flow in complex geometries. *Journal of Computational Physics*, 171:132–150, 2001.

10. C.S. Kueny. Embedded curved boundaries and adaptive mesh refinement. Technical Report UCRL-JC-129729, Lawrence Livermore Nat. Lab., 1998.

11. R.J. LeVeque and Zhilin Li. The immersed interface method for elliptic equations with discontinuous coefficients and singular sources. *SIAM Journal on Numerical Analysis*, 31(4):1019–1044, 1994.

12. R.J. LeVeque and Zhilin Li. Immersed interface methods for Stokes flow with elastic boundaries or surface tension. *SIAM Journal on Scientific Computing*, 18(3):709–735, 1997.

13. Z. Li. *The Immersed Interface Method - A Numerical Approach for Partial Differential Equations with Interfaces*. PhD thesis, University of Washington, 1994.

14. J. Nitsche. Über ein Variationsprinzip zur Lösung von Dirichlet Problemen bei Verwendung von Teilräumen die keinen Randbedingungen unterworfen sind. *Abh. Math. Sem. Univ. Hamburg*, 36:9, 1971.

15. C.S. Peskin. Numerical analysis of blood flow in the heart. *J. Comp. Phys.*, 25:220 – 252, 1977.

16. C. Tu and C. S. Peskin. Stability and instability in the computation of flows with moving immersed boundaries: A comparison of three methods. *SIAM Journal on Scientific and Statistical Computing*, 13:1361–1376, 1992.